Modelling Unsteady Two-Dimensional Hydromagnetic Flow of Micropolar Nanofluid along a Vertical Surface

ABSTRACT

Micropolar nanofluid synergizes both the properties of the micropolar fluid and those of nanofluid. They possess microstructural properties that permit both translational and rotational motion coupled with enhanced thermal conductivity due to the presence of nanoparticles. They have plethora of applications in electronic cooling, coolants in car radiators, working fluid in shell and tube heat exchangers, Lubrication, and in medical use (drug delivery, and cancer treatment). The study examines the effect of magnetic field strength, micropolar parameter, reaction rate, and Schmidt number on the velocity profile, temperature profile, and solute concentration by modelling the unsteady two dimensional Hydromagnetic flow of a micropolar nanofluid along a vertical plate. The magnetic field is imposed perpendicular to the flow. The equations and the accompanying boundary conditions governing the flow are formulated. The gyration and the inertial effect due to the micropolar fluid is infused into the body forces of the momentum equation. The introduction of similarity transformation variables converts the equations to nonlinear systems. The deployment of the state-space method linearizes the ordinary differential equations which numerically solves using the fourth-order Runge-Kutta method with a shooting technique in MATLAB. The bvp5c function is invoked. The outputs of the simulation are displayed graphically. The primary and secondary velocities decays with a climb in magnetic field due to the upsurge in Lorentz force. The climb in micropolar fluid parameter dampens the flow due to build up in viscous resistance as a result of increase in micro-rotational motion

within the flow. The solute concentration and temperature are declined with elevation in the reaction rate. Enhanced reaction rate consumes the reactants and thermal energy during the reaction process resulting in less solute concentration and low temperature. The Schmidt number lowers solute concentration and upsurges the fluid temperature.

.....

1. Introduction

Heat transfer fluids serve as a medium of dissipating heat in industrial processes. Traditional coolants such as water, ethylene glycol and engine oil have inherent poor thermal properties hindering their use in heat transfer processes. Studies shows that the thermal properties of these fluids can be enhanced by introducing particles of diameter ranging from $(1 - 100nm)$ (Danook et al., 2018; Okello et al., 2020; Younes et al., 2022). Nano-engineered fluids (nanofluids) have been successfully used as coolants in electronic devices, transformers, data centres, solar energy harvesting, oil recovery, aerodynamics, Lubrication and tribology, and in medical use (Erdi Korkmaz & Kumar Gupta, 2024; Hamad et al., 2024; Liang et al., 2025; Sheikhpour et al., 2020). Nano-based micropolar fluids simultaneously combines the properties of micropolar fluids (micro-rotational motion) and those of nanofluids (superior thermal conductivity). Several studies have been conducted on micropolar nanofluids to advance their use. Study by (Abbas et al., 2024) reported a decline in fluid velocity for the velocity slip parameter, a reduction in micro-rotational profile due to micro-rotation parameter, and upsurge in heat transfer due to Brownian and thermophoresis parameters. Examination into MHD flow of a micropolar nanofluid by (Ajala & Adegbite, 2023) revealed elevation in temperature profile with a climb in thermal radiation, Brownian motion, and thermophoresis, and a decline in velocity profile and concentration with a rise in inclination angle and chemical reaction respectively. The investigation by (Fatunmbi & Aako, 2025) observed decline in skin friction coefficient with increase in the micropolar parameter. The vortex viscosity term amplified the couple stress profile, whereas the thermophoresis, Brownian motion, and Peclet

number grew the thermal field. Research by (Shamshuddin et al., 2025) revealed increment in Brownian motion and thermophoresis elevated the concentration profile, whereas augmenting chemical reaction rate and Lewis number diminished the concentration profile. The fluid speed increased with increment in micropolar parameter. They also observed amplification in fluid temperature with radiation, Darcy term, and heat source and a decline in the same with climb in micropolar parameter. The numerical study by (Mkhatshwa, 2025) reported enhancement in species concentration with activation energy, variable mass diffusivity, thermal-diffusion, and solutal boundary effects, and a reduction in mass transportation rate with rise in thermal-diffusion and activation energy. Examination into micropolar effects by (Saranya et al., 2025) on nanofluid flow between two disks reported enhanced thermal conductivity, and viscosity leading to improved heat transfer efficiency. Nanoparticles presence elevated velocity and micro-rotation profiles resulting in more streamlined flow. The investigations by (Shah, 2025) recorded increment in velocity with a rise in mixed convection variable and modified Hartman number. The thermal flow behavior was enhanced with growth in radiation factor, thermophoresis number, the Biot number, and the Brownian motion magnitude. The research done by (Faisal et al., 2025) noted a decline in skin friction coefficient with a rise in rotation parameter. The Eckert number advanced the fluid temperature and dampened the primary microrotation. The fluid velocity and microrotation profiles were elevated with increase in vortex viscosity. From the aforementioned, a study on the unsteady two-dimensional Hydromagnetic flow of micropolar nanofluid along a vertical plate will be a meaningful contribution to literature in helping advance nanofluid use in various industrial and engineering processes.

2. Mathematical Formulation

A two-dimensional unsteady Hydromagnetic free convection flow of a nano-based micropolar fluid along a vertical plate with a uniform surface temperature T_w, a uniform upstream velocity, pressure and temperature is considered. The pressure velocity outside the viscous boundary layer varies with distance x along the plate such

that $u_\infty = Cx$ as shown in the diagram. The magnetic field $B = B_0 x^{\left(\frac{m-1}{2}\right)}$ is applied normal to the x-axis as illustrated in the diagram. The following assumptions are made:

i. The magnetic Reynolds number is small enough to neglect the induced magnet field.
ii. The flow is symmetrical over the wedge of constant angle $\pi\beta$.
iii. The surface temperature T_W is constant.
iv. Both pressure and velocity outside the viscosity boundary layer vary with distance x along the wedge.

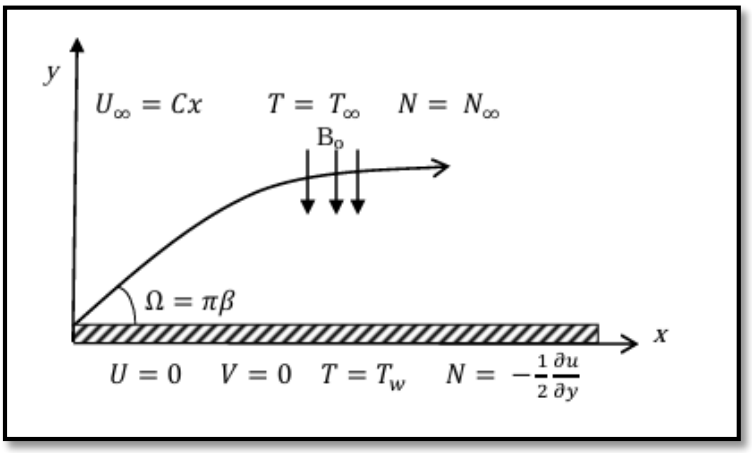

Figure 1: Flow configuration and coordinate system

Considering the assumptions and incorporating the models from (Buongiorno, 2005; Eringen, 1966) the conservation of mass equation, momentum equation, microrotation equation, energy equation, and concentration equation governing the flow are stated as;

Mass equation $$\frac{\partial u}{\partial x} + \frac{\partial v}{\partial y} = 0 \qquad (1)$$

Momentum equation

$$\frac{\partial u}{\partial t} + u\frac{\partial u}{\partial x} + v\frac{\partial v}{\partial y} = \frac{\partial u_\infty}{\partial t} + u_\infty \frac{\partial u_\infty}{\partial x} + \left(\frac{\mu + s}{\rho}\right)\frac{\partial^2 u}{\partial y^2} + \frac{s}{\rho}\frac{\partial N}{\partial y} + \frac{\sigma B^2(x)(u_\infty - u)}{\rho} \quad (2)$$

Microrotation equation

$$\frac{\partial N}{\partial t} + u\frac{\partial N}{\partial x} + v\frac{\partial N}{\partial y} = \left(\frac{\gamma}{j\rho}\right)\frac{\partial^2 N}{\partial y^2} - \left(\frac{s}{j\rho}\right)\left(2N + \frac{\partial u}{\partial y}\right) \quad (3)$$

Energy equation

$$\frac{\partial T}{\partial t} + u\frac{\partial T}{\partial x} + v\frac{\partial T}{\partial y} = \alpha\frac{\partial^2 T}{\partial y^2} + \tau\left(D_B\frac{\partial C}{dy}\frac{\partial T}{\partial y} + \frac{D_T}{T_\infty}\left(\frac{\partial T}{\partial y}\right)^2\right) \quad (4)$$

Concentration equation

$$\frac{\partial C}{\partial t} + u\frac{\partial C}{\partial x} + v\frac{\partial C}{\partial y} = D_B\frac{\partial^2 C}{\partial y^2} + \frac{D_T}{T_\infty}\frac{\partial^2 T}{\partial y^2} - k(C - C_\infty) \quad (5)$$

The equations $(1-5)$ are subject to the boundary conditions $6(a-b)$

$$u = 0, \qquad v = 0\,, \qquad N = -\frac{1}{2}\frac{\partial u}{\partial y},$$

$$T = T_W\,,\ D_B\frac{\partial C}{dy} + \frac{D_T}{T_\infty}\frac{\partial T}{\partial y} = 0 \ \ at\ \ y = 0 \ \ \ t = 0. \quad (6a)$$

$$u(\infty, t) \to u_\infty,\ N(\infty, t) \to 0,\ T(\infty, t) \to T_\infty,\ C \to C_\infty \ \ as\ y \to \infty,\ \ t > 0 \quad (6b)$$

Where u and v are the velocities in x and y direction respectively, B is the magnetic current, σ is the Stefan-Boltzman constant and ρ is the density of the micropolar nanofluid, $u_\infty = cx$ is the stream velocity, N is the microrotation vector normal to $x - y$ plane , T is the temperature of the fluid, T_W is the temperature of the wall, j is microrotation density, γ is microrotation constant, D_B is Brownian diffusion coefficient, D_T is the thermosphoresis diffussion coefficient, s is the vortex viscosity, μ is the dynamic viscosity, C is the ambient concentration at

any reference point, C_W is variable concentration and τ is the ratio of the effective heat capacity of the base fluid to the effective heat capacity of the micropolar fluid.

2.1 Non-dimensionalization

The equations $(1-5)$ and the boundary conditions $6(a-b)$ are expressed in dimensionless form by introducing the similarity variables defined as

$$\eta = \left(\frac{(m+1)u_\infty(x)}{2vx}\right)^2 y, \quad \psi(x,y,t) = \left(\frac{2vxu_\infty(x)}{m+1}\right)^{\frac{1}{2}} f(\eta)$$

$$N(\eta) = u_\infty(x)\left(\frac{m+1}{2vx}\right)^{\frac{1}{2}} h(\eta),$$

$$\theta(\eta) = \frac{T-T_\infty}{T_W-T_\infty}, \phi(\eta) = \frac{C-C_\infty}{C_\infty} \tag{7}$$

The dimensionless equations are;

$$(1+S)f'''(\eta) + \frac{1}{2}(1-\xi)\eta f''(\eta) + Kh'(\eta) + \xi\left(M\left(1-f'(\eta)\right) - \left(f'(\eta)\right)^2 + f(\eta)f''(\eta) + 1\right) = 0. \tag{8}$$

$$\left(1+\frac{1}{2}S\right)h''(\eta) - S\xi\left(2h(\eta) + f''(\eta)\right) + \frac{1}{2}(1-\xi)\left(\eta h'(\eta) + h(\eta)\right) - \xi\left(f'(\eta)h(\eta) - f(\eta)h'(\eta)\right) = 0 \tag{9}$$

$$\theta''(\eta) + N_b\phi'(\eta)\theta'(\eta) + N_t\left(\theta'(\eta)\right)^2 + Pr\left(\frac{1}{2}\eta(1-\xi)\theta'(\eta) - \xi f'(\eta)\theta(\eta) + \xi f(\eta)\theta'(\eta)\right) = 0 \tag{10}$$

$$\phi''(\eta) + \frac{N_t}{N_b}\theta''(\eta) + Sc\left(-\xi s^*\phi(\eta) + \frac{1}{2}\eta(1-\xi)\phi'(\eta) - \xi\phi(\eta)f'(\eta) + \xi\phi'(\eta)f(\eta)\right) = 0. \tag{11}$$

With the initial and boundary conditions

$$f'(0) = 0, \quad f(0) = 0, \quad 2f(0) + f''(0) = 0,$$

$$\theta(0) = 0, \qquad \phi'(0) + \frac{N_t}{N_b}\theta'(0) = 0.$$

$$f'(\infty) \to 1, \quad h(\infty) \to 0, \quad \theta(\infty) \to 0, \quad \phi(\infty) \to 0, \tag{12}$$

Where;

$$N_b = \frac{\tau D_B C_0 x}{\alpha}, \quad N_t = \frac{\tau D_T}{T_\infty}\frac{T_0 x}{\alpha}, \quad Pr = \frac{\vartheta}{\alpha}, \quad \frac{s}{\mu} = S, \quad M = \frac{\sigma B^2}{a\rho},$$

$$\frac{s}{a} = S^*, \quad Sc = \frac{\vartheta}{D_B}$$

Where $N_b$is the thermophoresis parameter, N_t is the Brownian parameter,Pr is the Prandtl number, M is the magnetic parameter, Sc is the Schmidt number, s^* is viscosity ratio, S is the material parameter.

3. Numerical Procedure

Letting

$$x_1 = f, \qquad x_2 = f', \qquad x_3 = f'', \qquad x_4 = h, \qquad x_5 = h',$$
$$x_6 = \theta, \qquad x_7 = \theta', \qquad x_8 = \phi, \qquad x_9 = \phi' \tag{13}$$

So, we have

$$x_1' = x_2, \qquad x_2' = x_3 \tag{14a}$$

$$x_3' = -\frac{1}{(1+S)}\left(\frac{1}{2}(1-\xi)\eta x_3 + Kx_5 + \xi(M(1-x_2) - x_2^2 + x_1x_3 + 1)\right) \tag{14b}$$

$$x_4' = x_5 \tag{14c}$$

$$x_5' = -\frac{1}{\left(1+\frac{1}{2}S\right)}\Bigg(-K\xi(2x_4+x_3)+\frac{1}{2}(1-\xi)(\eta x_5+x_4) - \xi(x_2x_4-x_1x_5)\Bigg) \tag{14d}$$

$$x_6' = x_7 \tag{14e}$$

$$x_7' = -\left(N_b x_7 x_9 + N_t x_7^2 + Pr\left(\frac{1}{2}\eta(1-\xi)x_7 - \xi x_2 x_6 + \xi x_1 x_7\right)\right) \tag{14f}$$

$$x_8' = x_9 \tag{14g}$$

$$x_9' = -\left(\frac{N_t}{N_b}x_7' + Sc\left(-\xi s x_8 + \frac{1}{2}\eta(1-\xi)x_9 - \xi x_8 x_2 + \xi x_9 x_1\right)\right) \tag{14h}$$

With the initial and boundary conditions

$$x_1(0) = 0, \qquad x_2(0) = 0, \quad 2x_1(0) + x_3(0) = 0,$$

$$x_6(0) = 0, \qquad x_9(0) + \frac{N_t}{N_b}x_7 = 0.$$

$$x_2(\infty) \to 1, \quad x_4(\infty) \to 0, \quad x_6(\infty) \to 0, \quad x_8(\infty) \to 0. \tag{15}$$

4. Results and Discussion

Figures 2 and 3 show the effects of the magnetic parameter M on the unsteady flow of the reactive micropolar fluid. The graphs show that there is a decrease in both primary and secondary velocities as magnetic field strength increases. As the magnetic field strength increases, the Lorentz force becomes more pronounced, acting as a

counterforce to the fluid's natural motion. In the realm of unsteady flow, where velocities and other flow characteristics are in constant flux, the implications of this decrease in velocity are profound. The reduced kinetic energy of the fluid hampers its ability to engage in effective convective heat transfer, leading to uneven temperature distributions. Similar results were obtained by (Rahman et al., 2013) in their study of Local similarity solution for unsteady 2D-forced convective flow heat and mass transfer flow along a wedge with thermophoresis.

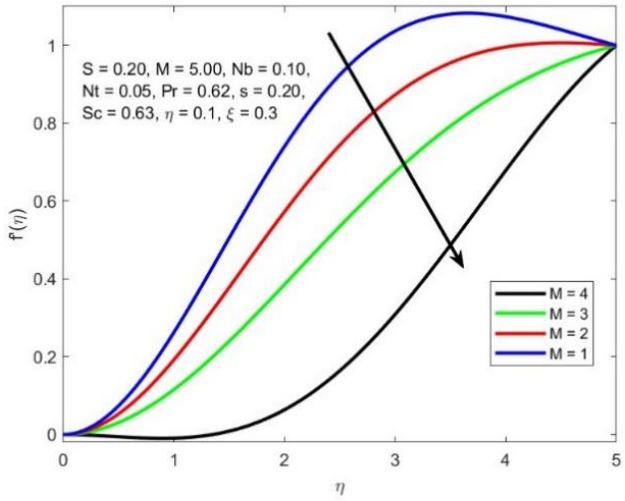

Figure 2: Effects of magnetic field strength on primary velocity

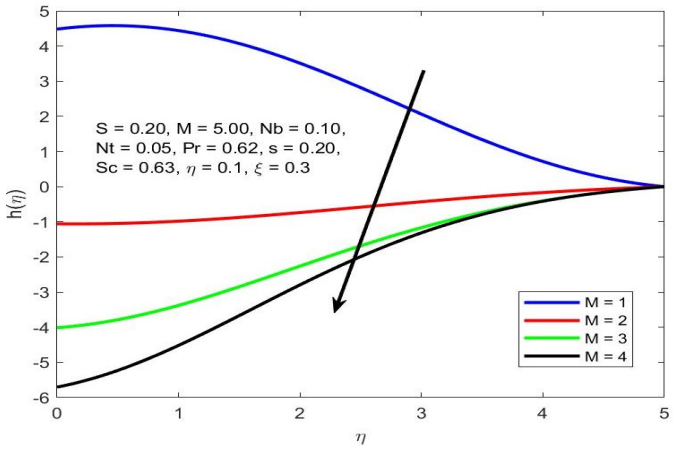

Figure 3: Effects of magnetic field strength on secondary velocity

Figures 4 and 5 present the effects of the micropolar fluid parameter on primary and secondary velocities in the unsteady flow of reactive micropolar fluids. In Figure 4, increasing the micropolar fluid parameter results in a decrease in primary velocity. This decline is due to the interaction between micro-rotational motion and the bulk flow of the fluid. The presence of micro-rotational effects introduces additional viscous resistance, thereby reducing the momentum of the primary flow

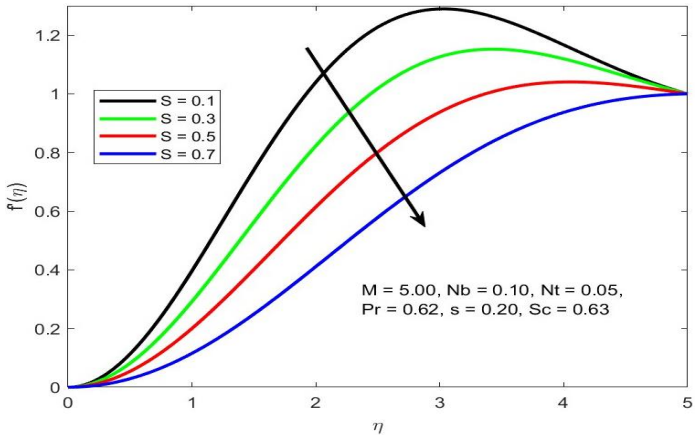

Figure 4: Effects of micropolar fluid parameter on primary velocity

Figure 5 shows a similar trend for secondary velocity, which also decreases with an increase in the micropolar fluid parameter. This reduction affects the circulation patterns within the fluid. A decrease in secondary velocity may hinder effective mixing and the uniform distribution of thermal and mass properties. In unsteady flow situations, where fluid behavior can change rapidly, the diminished secondary flow can result in less efficient transport of energy and solutes.

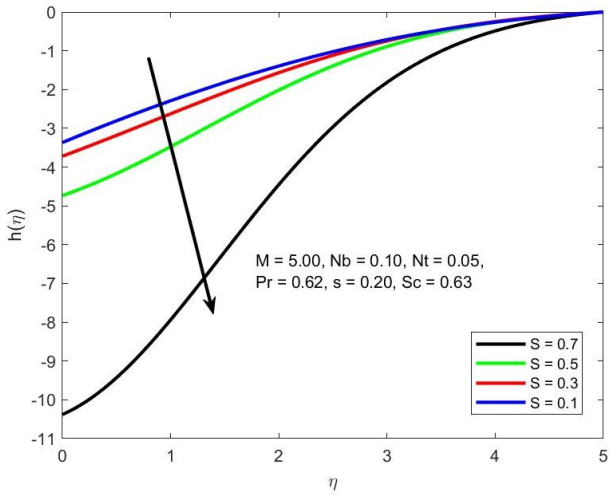

Figure 5: Effects of micropolar fluid parameter on secondary velocity

Figures 6 and 7 illustrate the effects of reaction rate on temperature and concentration in the unsteady flow of reactive micropolar fluids. As shown in Figure 6, an increase in the reaction rate leads to a decrease in temperature. This inverse relationship arises from the consumption of thermal energy during the reaction process, where the transformation of reactants into products can absorb energy, resulting in a lower overall temperature in the fluid. These results concur with those found by (Damseh et al., 2007) in the study of Unsteady natural convection heat transfer of micropolar fluid over a vertical surface with constant heat flux.

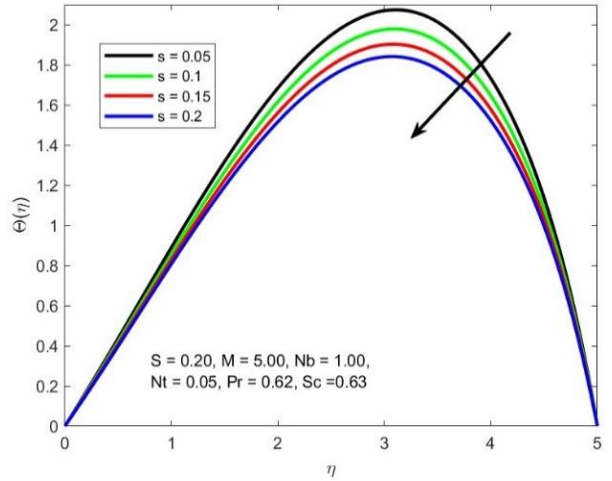

Figure 6: Effects of reaction rate on temperature

Figure 7 indicates that a higher reaction rate also results in a decrease in solute concentration. This decrease occurs because the reactants are consumed more rapidly than they can be replenished within the fluid. In unsteady flow conditions, where concentrations can vary significantly, this can lead to localized depletion of reactants, potentially impacting the efficiency of the reaction.

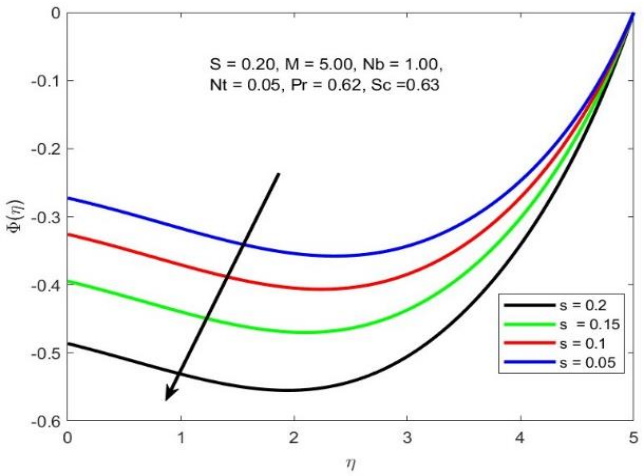

Figure 7: Effects of reaction rate on concentration

Figures 8 and 9 illustrate the effects of the Schmidt number on concentration and temperature in the unsteady flow of reactive micropolar fluids. In Figure 8, an increase in the Schmidt number results in a decrease in solute concentration. The Schmidt number quantifies the relative rates of momentum and mass diffusion in a fluid. A higher Schmidt number indicates that the viscous forces dominate over the diffusion processes, which can hinder the transport of solutes. As a result, the effective mixing of the fluid decreases, leading to localized areas of lower concentration as the solutes are not evenly distributed throughout the fluid.

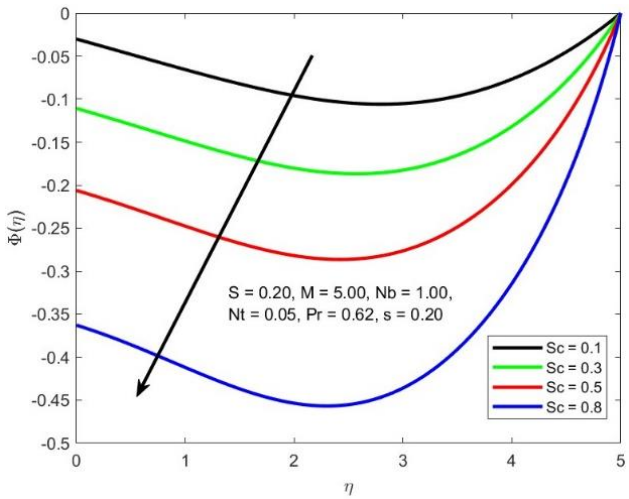

Figure 8: Effects of Schmidt number on concentration

In Figure 9, the increase in the Schmidt number is associated with an increase in temperature. This phenomenon can be explained by the reduced mass transfer efficiency linked to higher Schmidt numbers. With diminished solute transport, the heat dissipation mechanisms become less effective, allowing the temperature to rise within the fluid. The fluid's ability to carry away heat diminishes as the slower diffusion of mass means that any thermal energy generated within the system remains trapped, leading to higher thermal profiles. These findings coincide with those of (Aurangzaib et al., 2013) in their study of Unsteady MHD mixed convection flow with heat and mass transfer over a vertical plate in a micropolar fluid-saturated porous medium.

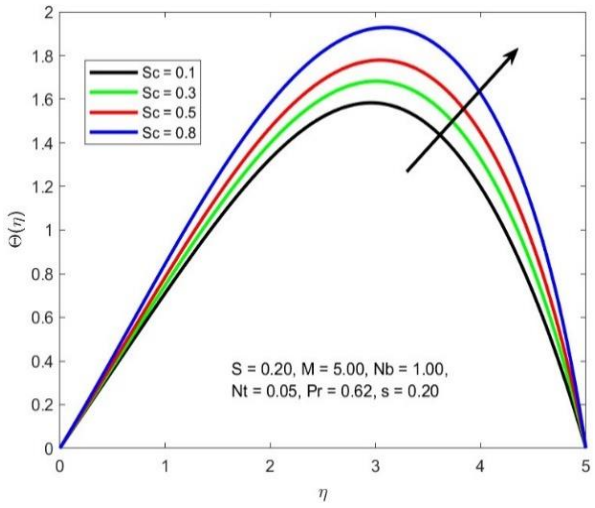

Figure 9: Effects of Schmidt number on temperature

5. Conclusion

This study modeled the unsteady two-dimensional Hydromagnetic flow of a micropolar nano-based fluid along a vertical plate subject to a constant magnetic field. The equations governing the flow were formulated and non-dimensionalized to determine the effects of magnetic fields, micropolar fluid properties, reaction rates, and the Schmidt number on the flow. The simulation was achieved using MATLAB. The following conclusions can be derived from the study:

i. The primary and secondary velocities decays with a climb in magnetic field due to the upsurge in Lorentz force.

ii. The climb in micropolar fluid parameter dampens the flow due to a buildup in viscous resistance as a result of increase in micro-rotational motion within the flow.

iii. The solute concentration and temperature are declined with elevation in the reaction rate. Enhanced reaction rate consumes the reactants and thermal energy during the reaction process resulting in less solute concentration and low temperature.

iv. The Schmidt number lowers solute concentration and elevates the fluid temperature.

Disclaimer (Artificial Intelligence)

Authors hereby declare that NO generative AI technologies such as Large Language Models (ChatGPT, COPILOT, etc) and text-to-image generators have been used during writing or editing of manuscripts.

REFFERENCES

Abbas, T., Khan, S. U., Saeed, M., Khan, M. I., Ismail, E. A. A., Awwad, F. A., & Abdullaeva, B. S. (2024). Thermal stability and slip effects in micropolar nanofluid flow over a shrinking surface: A numerical study via Keller box scheme with block-elimination method. *AIP Advances*, *14*(8), 085102.

Ajala, O. A., & Adegbite, P. (2023). Hydromagnetic flow of micropolar nanofluids with co-effects of thermal radiation and chemical reaction over an inclined permeable stretching surface. *Beni-Suef University Journal of Basic and Applied Sciences*, *12*(1), 86.

Aurangzaib, A. R. M. Kasim, N. F. Mohammad, & Sharidan Shafie. (2013). Unsteady MHD Mixed Convection Flow with Heat and Mass Transfer over a Vertical Plate in a Micropolar Fluid-Saturated Porous Medium. *Journal of Applied Science and Engineering*, *16*(2), 141–150.

Buongiorno, J. (2005). Convective Transport in Nanofluids. *Journal of Heat Transfer*, *128*(3), 240–250.

Damseh, R. A., Al-Azab, T. A., & Shannak, B. A. (2007). Unsteady Natural Convection Heat Transfer of Micropolar Fluid over a Vertical Surface with Constant Heat Flux. *Turkish Journal of Engineering and Environmental Science*, *31*(4), 225–233.

Danook, S. H., Jasim, Q. K., & Hussein, A. M. (2018). Nanofluid Convective Heat Transfer Enhancement Elliptical Tube inside Circular Tube under Turbulent Flow. *Mathematical and Computational Applications*, *23*(4), 78.

Erdi Korkmaz, M., & Kumar Gupta, M. (2024). Nano lubricants in machining and tribology applications: A state of the art review on challenges and future trend. *Journal of Molecular Liquids*, *407*, 125261.

Eringen, A. (1966). Theory of Micropolar Fluids. *Indiana University Mathematics Journal*, *16*(1), 1–18.

Faisal, M., Ganie, A. H., Badruddin, I. A., & Zedan, A. S. A. H. (2025). Exponentially stretched flow of radiative micropolar hybrid nanofluid with dissipative energy using BVPh 2.0. *ZAMM - Journal of Applied Mathematics and Mechanics / Zeitschrift Für Angewandte Mathematik Und Mechanik*, *105*(6), e70115.

Fatunmbi, E. O., & Aako, O. L. (2025). Thermodynamic Analysis of Hydromagnetic Micropolar Nanofluid Flow with Viscous Dissipation and Non-Uniform Heat Source in a Porous Channel. *Journal of Engineering Research and Reports*, *27*(3), 285–298.

Hamad, N. H., Adham, A. M., & Abdullah, R. S. (2024). Cooling electronic components by using nanofluids: A review. *Journal of Thermal Analysis and Calorimetry*, *149*(22), 12503–12514.

Liang, F., Wang, W., Zhu, S., Hu, Y., Zhao, Z., Tan, Y., Yu, G., Hou, J., & Li, J. (2025). Nanofluids application in enhanced oil recovery process-opportunities and challenges. *Arabian Journal of Chemistry*, *18*(1), 106053.

Mkhatshwa, M. P. (2025). Numerical study of Ellis-micropolar tetra-hybrid nanofluid flow over a stretching surface with g-jitter and magnetic dipole. *Multiscale and Multidisciplinary Modeling, Experiments and Design*, *8*(10), 450.

Okello, J. A., Mutuku, W. N., & Oyem, A. O. (2020). A Review of Nanofluids Synthesis, Factors Influencing Their Thermophysical Properties and Applications. *Journal of Engineering Research and Reports*.

Rahman, Atm. M., Alam, M. S., Alim, M. A., & Chowdhury, M. K. (2013). Unsteady MHD Forced Convective Heat and Mass Transfer Flow along a Wedge with Variable Electric Conductivity and Thermophoresis. *Procedia Engineering*, *56*, 531–537.

Saranya, S., Ragupathi, P., & Al-Mdallal, Q. M. (2025). Impact of micropolar effects on nanofluid flow between two disks. *International Journal of Thermofluids*, *26*, 101050.

Shah, N. A. (2025). Stagnation point on the micropolar bioconvection nanofluid flow over inclined Riga plate: Keller box analysis. *Physics of Fluids*, *37*(1), 012013.

Shamshuddin, MD., Gamar, F., Salawu, S. O., & Reddy, B. P. (2025). Two-phase micropolar nanofluid flow in an isothermal extending porous sheet with heat radiation and chemical interaction: Numerical study. *Partial Differential Equations in Applied Mathematics*, *14*, 101226.

Sheikhpour, M., Arabi, M., Kasaeian, A., Rokn Rabei, A., & Taherian, Z. (2020). Role of Nanofluids in Drug Delivery and Biomedical Technology: Methods and Applications. *Nanotechnology, Science and Applications*, *13*, 47–59.

Younes, H., Mao, M., Sohel Murshed, S. M., Lou, D., Hong, H., & Peterson, G. P. (2022). Nanofluids: Key parameters to enhance thermal conductivity and its applications. *Applied Thermal Engineering*, *207*, 118202.